Chemical State Study of Palladium Powder and Ceria-Supported Palladium during Low-Temperature CO Oxidation

Seung-Hoon Oh and Gar B. Hoflund*

Department of Chemical Engineering, University of Florida, Gainesville, Florida 32611

Received: January 20, 2006; In Final Form: April 12, 2006

The chemical state of Pd at the surfaces of two sizes of Pd powders and ceria-supported Pd during low-temperature CO oxidation has been studied using X-ray photoelectron spectroscopy (XPS). During oxidation in O_2, metallic Pd powder is converted into PdO, and the thickness of the PdO layer increases with increasing reaction temperature. A similar Pd oxidation process occurs during the catalytic CO oxidation reaction, but the extent of the Pd oxidation is less due to the presence of CO which is a reducing agent. The reaction rate data indicate that the larger size Pd powder is about three times more active than the smaller size Pd powder on a surface area basis at 160 °C. Catalytic CO oxidation data obtained from 10 wt % Pd supported on nanocrystalline ceria powder indicate that there is a strong chemical interaction between the ceria and the supported Pd. The Pd is present as PdO on the fresh catalyst. During reaction, small amounts of Pd metal and PdO_2 are formed at 50 °C while less Pd metal and only a small amount of PdO_2 are present after running the reaction at 110 °C. At 50 °C, the catalytic activity decays rapidly due to accumulation of carbonate or bicarbonate species on the surface. This decay does not occur at 110 °C due to decomposition of the bicarbonate species.

Introduction

The development of low-temperature carbon monoxide oxidation catalysts has been an active research area for many years due to the many important environmental and technological applications including closed-cycle CO_2 pulsed lasers, CO gas detection sensors, air-purification, gas masks, and polymer electrolyte fuel cells.[1−4] Many different types of catalysts have been tested for low-temperature CO oxidation. Most of the catalysts that exhibit high activity consist of one or more noble metals dispersed on a reducible oxide support (NMRO catalysts).[1] There are many variables involved in the preparation, pretreatment, and reaction which all significantly affect the catalytic activity and decay behavior of the different catalysts. Supported platinum[5] and gold[6−8] catalysts were originally proposed for low-temperature CO oxidation. Since then, other noble metals including palladium, rhodium, and ruthenium have received attention for CO oxidation.[4] A review of platinum-based and gold-containing NMRO catalysts was published by Hoflund and Epling,[9] and a review of gold-containing catalysts was published by Haruta and Date.[10]

Palladium-based catalysts which contain Pt and Rh are widely used for automotive three-way catalysts which can simultaneously remove nitric oxides, carbon monoxide, and hydrocarbons. These catalysts have better durability for the treatment of automotive exhaust than platinum or rhodium. Automotive catalysts which contain only Pd have been proposed recently as an alternative for the industry. Most Pd-containing catalysts used in CO oxidation studies and surface characterization studies were supported on metal oxides such as Al_2O_3, SiO_2, TiO_2, CoO_x, CeO_2, or zeolites. The influence of these different metal oxides on low-temperature CO oxidation has been reported by Pavlova and co-workers.[11] They found that the CO activities for Pd supported on different metal oxides (SiO_2, TiO_2, and Al_2O_3) vary considerably and attribute this to varying densities of surface defect centers which can stabilize CO and O_2. Hoffmann et al.[12] have studied Pd size effects for CO oxidation over Al_2O_3-supported Pd. They found that two different Pd particle sizes (1.8 and 5.5 nm) exhibit different transient and steady-state kinetics using molecular beam experiments.

Three catalysts which perform very well for low-temperature CO oxidation are iron-oxide-supported Au,[6] platinized tin oxide,[5,9] and manganese-oxide-supported gold.[13,14] Au/MnO_x is an excellent catalyst when the CO_2 concentration is low[15,16] while Fe-stabilized Pt/SnO_x performs well in a CO_2-rich environment.[17] Au supported on titania has drawn attention recently from a fundamental viewpoint,[18−20] but this catalyst is of little technological interest due to its high activity decay rate.[21] In a more recent study by Oh and Hoflund,[22] Pd supported on MnO_x, CeO_2, TiO_2, CoO_x, and Al_2O_3 have been examined for CO oxidation activity near stoichiometric conditions. Of these catalysts, 10 wt % Pd/CeO_2 performed the best. In this present study, the chemical state of Pd has been determined using X-ray photoelectron spectroscopy (XPS) for two sizes of Pd powders and 10 wt % Pd supported on nanocrystalline ceria. Apparently, CO oxidation has not been studied over Pd metal powder. This eliminates the influence of the Pd-oxide support interaction so that the chemistry of this simpler system can be examined. Hopefully, this study will form a basis to understand the more complex catalytic systems for CO oxidation.

Experimental Section

Several types of catalysts were examined in this study. Two different sizes of Pd metal powder (99.95% purity on a metal basis) were purchased from Alfa Aesar. One had a size range from 0.25 to 0.55 μm with a BET surface area of 10.6 m^2/g, and the other had a size range from 1 to 1.5 μm with a BET

* To whom correspondence should be addressed. Fax: 352-392-9513. E-mail: garho@hotmail.com.

10.1021/jp060435u CCC: $33.50
Published on Web 06/01/2006

surface area of 1.08 m^2/g. An impregnated 10 wt % Pd/CeO_2 catalyst (BET surface area of 43.2 m^2/g) was prepared using the incipient wetness method in which palladium nitrate ($Pd(NO_3)\cdot H_2O$) was added to nanocrystalline ceria (CeO_2, Nano-Phase, Inc., BET surface area of 50.7 m^2/g) using purified water. The catalyst was dried for 5 h in an oven at 100 °C and calcined in air at 280 °C for 3 h. This temperature is high enough to decompose the Pd precursor as evidenced by the absence of a N 1s peak in XPS spectra obtained from the fresh catalyst. The catalyst was granulated into fine particles using a mortar and pestle. A 10 wt % $Pd-CeO_2$ mixture was prepared by physically combining Pd metal (0.25 to 0.55 μm) and nanocrystalline ceria in a 1:9 weight ratio of Pd to ceria. This physical mixture has a BET surface area of 46.7 m^2/g.

The reaction studies were performed in a tubular reactor system operating at atmospheric pressure. A specified mass of each catalyst was supported by glass wool in a quarter-inch diameter quartz U-shaped tube. The tube was then inserted in a Thermolyne 21100 furnace. A K-type thermocouple was placed around the U-tube at the center of the catalyst bed and connected to an auto-tuning PID controller. The reaction temperature was maintained accurately inside the furnace within ±1 °C. Ultrahigh purity test gases obtained from Praxair were mixed to yield a composition about 1% CO and 0.5% O_2 in helium. The feed stream was slightly oxygen rich by less than 150 ppm due to small fluctuations of flow rates. The total flow rate was 45 cm^3/min. Initially, the gas stream was bypassed and analyzed in a Hewlett-Packard 5890A gas chromatograph to determine the feed concentration. For product analysis, a 5A molecular sieve column was connected to a thermal conductivity detector (TCD). Their temperatures were kept essentially constant at 80 and 150 °C, respectively. The reaction gas stream and bypass gas line were connected to a Valco 6 port valve with a 1 cm^3 sample loop. The conversion of CO was calculated using the peak area differences between the unreacted bypass and the effluent from the catalyst bed. During reaction, care was taken to allow the temperature to equilibrate before a sample of the outlet gas was analyzed. Multiple samples were taken and averaged to ensure that the catalytic system had reached steady state.

Surface characterization studies were carried out on the catalysts before and after oxidation or reaction at various temperatures. The catalyst powders were pressed into aluminum cups, inserted into the ultrahigh vacuum chamber and characterized using XPS. XPS was performed using a double-pass cylindrical mirror analyzer (DPCMA, PHI Model 25-255AR) and pulse counting detection[23] by operating the DPCMA in the retarding mode using a pass energy of 25 eV for the high-resolution spectra and 50 eV for the survey spectra. The X-rays were generated using a Mg Kα X-ray source. Model experiments were performed to ensure that the brief exposure to air during the transfer from the catalytic reactor to the characterization chamber does not alter the Pd chemical state.

Results and Discussion

Pd Powders. The catalytic activities of the two Pd metal powders for CO oxidation as a function of temperature are shown in Figure 1. The Pd powders were initially given a reductive pretreatment in 3.5% H_2 at 100 °C for 1 h to ensure that the Pd was metallic. This state is referred to as the fresh catalyst for the Pd metal powders. As shown below, the Pd metal powder develops Pd oxide at the surface after either oxidative treatments or exposure to catalytic reaction conditions. Both the 0.25−0.55 μm and the 1−1.5 μm powders exhibit poor CO oxidation activity below 150 °C. The smaller size Pd powder is more active above 150 °C and reaches complete conversion at 180 °C while the larger size Pd powder oxidizes only 15% of the CO at this temperature and does not reach complete conversion until about 250 °C. The complete conversion of CO corresponds to oxidation of 1.87×10^{-5} gmole/min of CO. The average areal reaction rates in gmole/min·m^2 have been calculated from the data in Figure 1 at 160 °C. On an areal basis, the large Pd powder (1.08 m^2/g) is 3.11 times more active than the small Pd powder (10.6 m^2/g) with average areal reaction rates of 0.53×10^{-6} and 0.17×10^{-6} gmole/min·m^2, respectively. This reaction is exothermic so 160 °C was chosen to minimize heat effects. The reason for the difference in the areal-based reaction rates is not known. It may be due to a size effect or more likely to surface morphological differences. The oxygen conversions over the whole temperature range (not shown) are essentially identical to the carbon monoxide conversions.

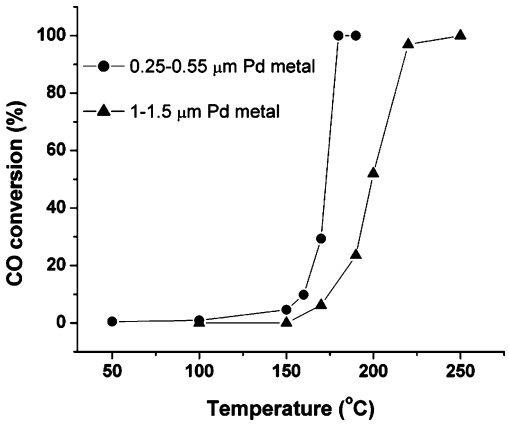

Figure 1. CO conversion as a function of temperature for two different size Pd metal powders. The feed stream was 1.0% CO and 0.5% O_2 in He at a total flow rate of 45 cm^3/min.

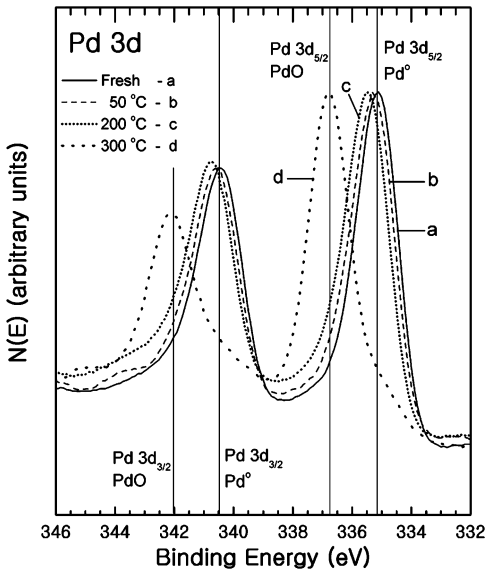

Figure 2. High-resolution XPS Pd 3d spectra obtained from (a) fresh Pd metal powder and Pd metal powder after exposure to 0.5% O_2 for 60 min in the reactor at (b) 50, (c) 200, and (d) 300 °C. All Pd powders were prereduced with 3.5% H_2 in He at 100 °C for 60 min.

The large Pd powder was then reduced in H_2 as described above to produce metallic Pd and then exposed to 0.5% O_2 in He for 1 h at 50, 200, and 300 °C. High-resolution XPS Pd 3d spectra obtained after these treatments are shown in Figure 2, and the corresponding O 1s and Pd 3p spectra are shown in

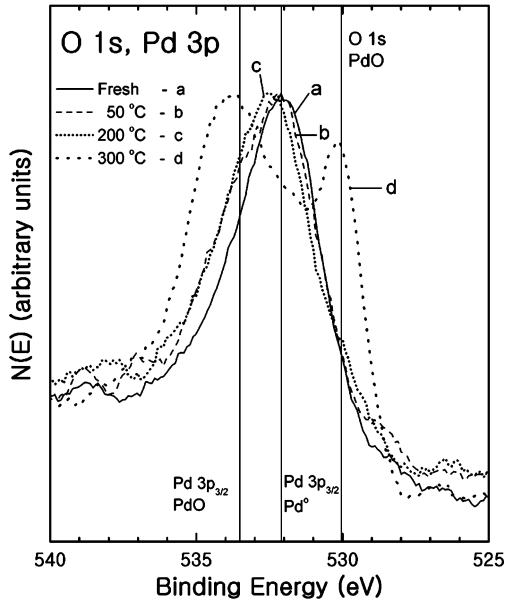

Figure 3. High-resolution XPS O 1s and Pd 3p spectra obtained from (a) fresh Pd metal powder and Pd metal powder after exposure to 0.5% O_2 for 60 min in the reactor at (b) 50, (c) 200, and (d) 300 °C. All Pd powders were prereduced with 3.5% H_2 in He at 100 °C for 60 min.

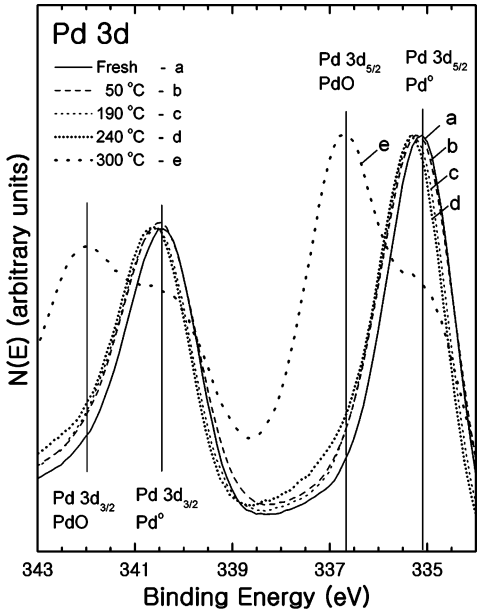

Figure 4. High-resolution XPS Pd 3d spectra obtained from (a) fresh Pd metal powder and Pd metal powder after exposure to 1% CO and 0.5% O_2 for 60 min in the catalytic reactor at (b) 50, (c) 190, (d) 240, and (e) 300 °C. The Pd powder was reduced with 3.5% H_2 in He at 100 °C for 60 min.

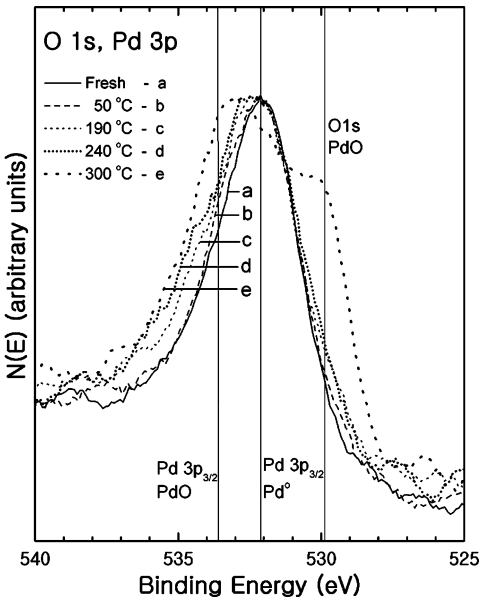

Figure 5. High-resolution XPS O 1s and Pd 3p spectra obtained from (a) fresh Pd metal powder and Pd metal powder after exposure to 1% CO and 0.5% O_2 for 60 min in the catalytic reactor at (b) 50, (c) 190, (d) 240, and (e) 300 °C. The Pd powder was reduced with 3.5% H_2 in He at 100 °C for 60 min.

Figure 3. The Pd 3d and Pd 3p features are characteristic of clean Pd with no Pd oxide present. After the O_2 treatment at 50 °C (Figure 2b), all of the features are altered. The Pd $3d_{5/2}$ and $3d_{3/2}$ peaks are shifted to higher binding energies (BEs) by about 0.3 eV, and they are broadened on the high-BE side. The Pd $3p_{3/2}$ peak is broadened to both the low-BE and the high-BE sides. The broadening on the low-BE side is due to the presence of an O 1s feature from PdO, and the broadening on the high-BE side is due to the formation of a PdO Pd 3p feature. These assertions are consistent with the broadening on the high-BE sides of the Pd 3d features and the shift toward PdO features in Figure 2. The changes in these features occur to a greater extent after the O_2 exposure at 200 °C (Figure 2c). The shift in the Pd 3d peaks are still small after the 200 °C-O_2 treatment so the corresponding changes in the O 1s and Pd 3p features shown in Figure 3c are also small. Nevertheless, a more well-defined O 1s shoulder is apparent after this treatment. This shoulder is particularly apparent in the same set of spectra which has not been normalized (not shown). After the O_2 exposure at 300 °C (Figure 2d), the spectral changes are quite large due to nearly complete conversion of Pd metal to PdO in the near-surface region. In Figure 2d, the predominant features are PdO 3d peaks and the small shoulders on the low-BE sides are small Pd metal features. Two predominant features are now present in Figure 3d due to PdO Pd 3p and PdO O 1s peaks. These data indicate that an oxide layer forms on the Pd particles and that the thickness of this oxide layer depends on the temperature. Oxidation of Pd occurs at lower temperatures, but the fact that the oxide layers remain thin indicates that diffusion of oxygen to the underlying Pd metal is the slow step in the oxidation process.

XPS data were also obtained after running the catalytic reaction over the large Pd powder at 50, 190, 240, and 300 °C. Before reaction, the catalysts were reduced in 3.5% H_2 in He for 1 h at 100 °C to ensure the presence of Pd metal. High-resolution Pd 3d spectra and Pd 3p/O 1s spectra are shown in Figures 4 and 5, respectively. Similar to the results for the O_2 treatment, Pd metal is oxidized during the catalytic reaction, but it is not oxidized to the extent as during the oxidation. This is most readily apparent by comparing the Pd 3d peaks obtained after the 300 °C-O_2 treatment in Figure 2d and those obtained after running the catalytic reaction at 300 °C in Figure 4e. The O_2 treatment results in much more complete oxidation of the Pd compared with the catalytic reaction. This is due to the fact the O_2 treatment is purely oxidative while the catalytic reaction is both oxidative and reductive due to the presence of both O_2 and CO, respectively. A significant portion of O_2 which would go toward oxidizing Pd metal to PdO is instead reacted with CO to produce CO_2 resulting in a slower rate of Pd oxidation.

Electron energy loss spectroscopy (ELS) has proven to be a useful technique for distinguishing between Pd metal and PdO.[24] Advantages of ELS over XPS are that the primary beam can be focused to a small size, depth sensitivity can easily be

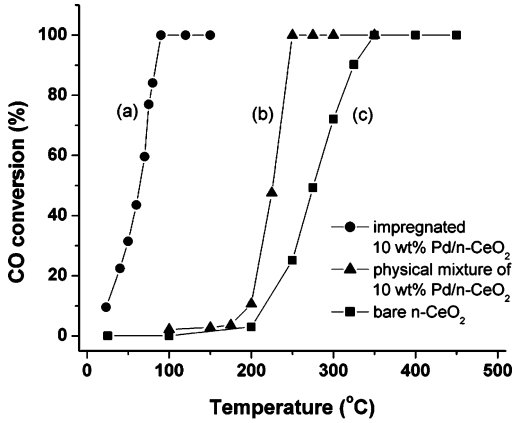

Figure 6. CO conversion as a function of temperature for (a) 10 wt % Pd/n−CeO_2 (impregnated), (b) a physical mixture of 0.010 g of Pd metal powder with sizes ranging from 0.25 to 0.55 μm and 0.090 g of nanocrystalline ceria, and (c) nanocrystalline ceria. The feed stream was 1.0% CO and 0.5% O_2 in He at a total flow rate of 45 cm^3/min.

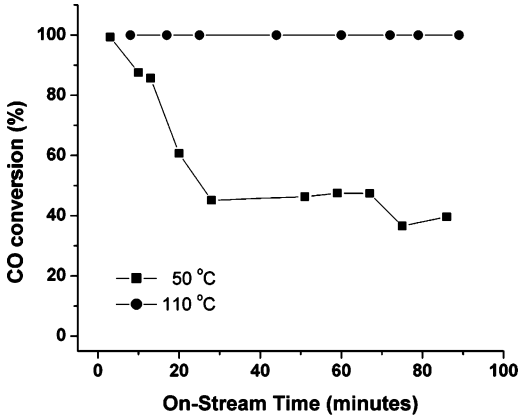

Figure 7. Conversion decay curves obtained from 10 wt % Pd/n−CeO_2 (impregnated) while operating the catalytic reactor at 50 and 110 °C.

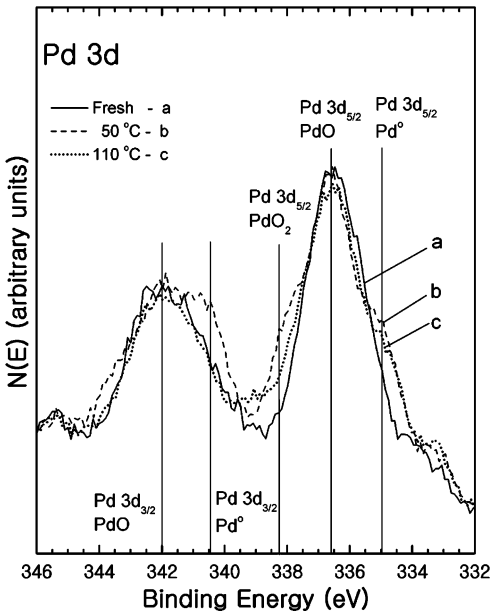

Figure 8. High-resolution XPS Pd 3d spectra obtained from (a) the fresh 10 wt % Pd/n−CeO_2, (b) the 10 wt % Pd/n−CeO_2 after 90 min reaction at 50 °C, and (c) after 90 min reaction at 110 °C. The feed stream was 1.0% CO and 0.5% O_2 in He at a total flow rate of 45 cm^3/min.

changed by varying the primary beam energy, and chemical state differences are often more apparent in ELS data. In a related study, ELS has been used to study H_2-reduced Pd powder after use as a catalyst for methane oxidation.[25] The results demonstrate that a shell of PdO develops on the Pd particles and that metallic Pd lies only beneath this shell. This implies that methane oxidation occurs on PdO. The fact that no Pd metal is present in the PdO layer indicates that an oxidative−reductive cycle ($Pd^0 \leftrightarrow Pd^{2+}$) is not responsible for low-temperature (<300 °C) methane oxidation. A proposed mechanism is that a methane C−H bond is broken, the C bonds to an O in PdO to form a methoxy species, and the H bonds to an O in PdO to form a hydroxyl species. The methoxy species then loses the other H atoms to form hydroxyl groups which combine and desorb as water molecules. The remaining C combines with 2O from PdO to form CO_2, which desorbs, and oxygen vacancies in the PdO layer. The last step is for these vacancies to adsorb O_2 to form PdO.

These are several important similarities between catalytic methane oxidation and catalytic CO oxidation including (1) O_2 is a reactant in both cases, (2) CO_2 is a product in both cases, and (3) both reactions occur over many of the same catalysts. The differences are that (1) the C≡O bond is not broken while all the C−H bonds are broken and (2) water is a product in methane oxidation. Since both reactants are usually run in an oxygen-rich environment, the presence of PdO on Pd powder formed during CO oxidation most likely is a shell over Pd metal as has been shown to be the case for methane oxidation.

Ceria-Supported Pd. CO conversion vs temperature curves are shown in Figure 6 for nanocrystalline ceria, a physical mixture of nanocrystalline ceria and Pd metal, and nanocrystalline ceria impregnated with Pd (10 wt %). Nanocrystalline ceria exhibits the lowest catalytic activity, but it does exhibit significant activity above 200 °C. Bare oxides generally are not very catalytically active at low temperatures, and their activities can be enhanced by the addition of metal powder or supported metal. When Pd metal powder is physically mixed with nanocrystalline ceria (0.010 g of Pd metal powder with size ranging from 0.25 to 0.55 μm and 0.090 g of nanocrystalline ceria), the catalytic activity is increased considerably achieving 100% conversion below 250 °C. The third curve in Figure 6 indicates that 10 wt % impregnated Pd/n−CeO_2 is much more active than either the bare ceria or the physical mixture of Pd powder and ceria. It exhibits activity at room temperature and reaches 100% conversion below 100 °C, which is before the other two catalysts exhibit any activity. The data shown in Figure 6 indicate that there is a chemical interaction between ceria and the supported Pd which has a very large effect on the catalytic properties. This increased catalytic activity may be due to a Pd size effect or a chemical interaction between the ceria and Pd or a combination of these effects.

Conversion decay curves are shown in Figure 7 for the impregnated 10 wt % Pd/n−CeO_2 catalyst (170 mg) while operating the reaction at 50 and 110 °C. At 50 °C, the activity decays rapidly from 100 to about 40% conversion after 23 min and then stabilizes near this value. Previous studies[9] have shown that this decay in activity is due to accumulation of bicarbonate species on the surface. Elimination of these species by heating or subjecting the catalyst to vacuum or an inert gas flow results in restoration of its high catalytic activity. However, at 110 °C, a high conversion (100%) is maintained over the period tested. This fact indicates that at 110 °C the bicarbonate species decompose to yield CO_2 thereby maintaining a catalytically active surface.

XPS data have been obtained from the 10 wt % Pd/n−CeO_2 catalyst before and after running the CO oxidation reaction at

50 and 110 °C. High-resolution XPS Pd 3d spectra are shown in Figure 8. The Pd 3d feature obtained from the fresh catalyst (Figure 8a) is narrow and well-defined with a BE characteristic of PdO. No other species including metallic Pd or PdO_2 are observable. The spectrum obtained after running the catalytic reaction at 50 °C (Figure 8b) is much broader due to a shoulder on the low-BE side due to metallic Pd and a shoulder on the high-BE side due to PdO_2. A distinct O 1s peak (not shown) due to bicarbonate is present. This is consistent with the decay in activity shown in Figure 7. The Pd 3d spectrum obtained from the catalyst after running the reaction at 110 °C (Figure 8c) indicates that less Pd metal is present. The peak due to bicarbonate is not present in the O 1s spectrum (not shown) which is consistent with the fact that the activity does not decay at 110 °C. Only a very small amount of PdO_2 is present. Most of the Pd is present as PdO which is believed to be the active catalytic species. The reactant gas mixture contains O_2 which is an oxidizing agent and CO which is a reducing agent. The XPS data indicate that a small amount of PdO is oxidized to PdO_2 and that a small amount of PdO is reduced to metallic Pd.

Summary

In this study, the catalytic behavior for low-temperature CO oxidation of two Pd metal powders and ceria-supported Pd have been examined as a function of temperature. XPS has been performed on these catalysts to determine the Pd chemical state before and after running catalytic CO oxidation at different temperatures. For comparison, oxidation experiments also have been carried out on the larger Pd powder. Model studies have been performed to ensure that the brief exposure to air during transfer from the catalytic reactor to the UHV characterization experiment do not alter the Pd chemical state.

In each case, the Pd powder was reduced in hydrogen to form metallic Pd as the starting point. The oxidation studies were carried out by exposing the Pd powder to O_2 in He at varying temperatures. This treatment forms a layer of PdO on the Pd particles, and the thickness of this layer depends on the reactor temperature. At 300 °C, the PdO layer is so thick that the underlying Pd metal signal is quite small.

Catalytic CO oxidation was carried out over the small and large Pd powders. The areal activity of the large Pd powder is about three times higher than that of the small Pd powder at 160 °C. Similar chemical state changes occur during reaction as in the oxidation case. Metallic Pd is converted to a layer of PdO but at a slower rate than for oxidation because CO is a reducing agent. A proposed mechanism for catalytic CO oxidation is that CO adsorbs to form carbonate or bicarbonate species which decompose to form CO_2. Then oxygen chemisorbs at the vacancies. In this mechanism, the active surface is a PdO surface which may have adsorbed carbonate or bicarbonate species and oxygen vacancies but no Pd metal.

Reaction studies indicate that bare ceria exhibits catalytic activity for CO oxidation above 200 °C. If impregnated with 10 wt % Pd, it becomes highly active between 0 and 100 °C due to a chemical interaction between ceria and Pd. There is no decay in activity at 110 °C while there is significant decay at 50 °C due to accumulation of carbonate or bicarbonate species on the surface. XPS data indicate that PdO is the only Pd species on the surface of the fresh catalyst. During reaction at 50 °C, both PdO_2 and Pd metal form. Carbonate or bicarbonate species also accumulate on the surface resulting in a rapid decay in activity. At 110 °C, the activity does not decay and the carbonate or bicarbonate species does not accumulate on the surface. A smaller amount of Pd metal is present on the surface as is a much smaller amount of PdO_2.

References and Notes

(1) Schryer, D. R., Hoflund, G. B., Eds. *Low-Temperature CO oxidation Catalysts for Long-Life CO_2 Lasers*; NASA Conference Publication 3076; NASA: Washington, DC, 1990.
(2) Srinivason, B.; Gardner, S. D. *Surf. Interface Anal*. **1998**, *26*, 1035.
(3) T-Sanchez, R. M.; Udea, A.; Tanaka, K.; Haruta, M. *J. Catal*. **1997**, *168*, 125.
(4) Oh, S.; Sinkevitch, M. *J. Catal*. **1993**, *142*, 254.
(5) Stark, D. S.; Crocker, A.; Stewart, G. J. *J. Phys. E: Sci. Instrum*. **1983**, *16*, 158.
(6) Haruta, M.; Yamada, N.; Kobayashi, T.; Iijima, S. *J. Catal*. **1989**, *115*, 301.
(7) Haruta, M.; Tsubota, S.; Kobayashi, T.; Kageyama, H.; Genet, M.; Delmon, B. *J. Catal*. **1993**, *144*, 175.
(8) Gardner, S. D.; Hoflund, G. B.; Upchurch, B. T.; Schryer, D. R.; Kielin, E. J.; Schryer, J. *J. Catal*. **1991**, *129*, 114.
(9) Hoflund, G. B.; Epling, W. S. *Recent Res. Dev. Catal*. **1996**, *1*, 31.
(10) Haruta, M.; Date, M. *Appl. Catal., A* **2001**, *222*, 427.
(11) Pavlova, S. N.; Sadykov, V. A.; Bulgakov, N. N.; Bredikhin, M. N. *J. Catal*. **1996**, *161*, 517.
(12) Hoffmann, J.; Meusel, I.; Hartmann, J.; Libuda, J.; Freund, H.-J. *J. Catal*. **2001**, *204*, 378.
(13) Gardner, S. D.; Hoflund, G. B.; Schryer, D. R.; Schryer, J.; Upchurch, B. T.; Kielin, E. J. *Langmuir* **1991**, *7*, 2135.
(14) Gardner, S. D.; Hoflund, G. B.; Davidson, M. R.; Laitinen, H. A.; Schryer, D. R.; Upchurch, B. T. *Langmuir* **1991**, *7*, 2140.
(15) Hoflund, G. B.; Gardner, S. D.; Schryer, D. R.; Upchurch, B. T.; Kielin, E. J. *Langmuir* **1995**, *11*, 3431.
(16) Hoflund, G. B.; Gardner, S. D.; Schryer, D. R.; Upchurch, B. T.; Kielin, E. J. *React. Kinet. Catal. Lett.* **1996**, *58*, 19.
(17) Hoflund, G. B.; Upchurch, B. T.; Kielin, E. J.; Schryer, D. R. *Catal. Lett*. **1995**, *31*, 133.
(18) Soares, J. M. C.; Morrall, P.; Crossley, A.; Harris, P.; Bowder, M. *J. Catal*. **2005**, *219*, 17.
(19) Park, E. D.; Lee, J. S. *J. Catal*. **1999**, *186*, 1.
(20) Maeda, Y.; Fujitani, T.; Tsubota, S.; Haruta, M. *Surf. Sci*. **2004**, *562*, 1.
(21) Konova, P.; Naydenov, A.; Venkov, Cv.; Mehandjiev, D.; Andreeva, D.; Tabakova, T. *J. Mol. Catal. A: Chem.* **2004**, *213*, 235.
(22) Oh, S.-H.; Hoflund, G. B. To be submitted for publication.
(23) Gilbert, R. E.; Cox, D. F.; Hoflund, G. B. *Rev. Sci. Instrum*. **1982**, *53*, 1281.
(24) Hagelin, H. A. E.; Weaver, J. F.; Hoflund, G. B.; Salaita, G. N. *J. Electron Spectrosc. Relat. Phenom.* **2002**, *124*, 1.
(25) Hoflund, G. B.; Hagelin, H. A. E.; Weaver, J. F.; Salaita, G. N. *Appl. Surf. Sci*. **2003**, *205*, 102.